CASE FILE
COPY

NASA TECHNICAL NOTE

NASA TN D-3351

NASA TN D-3351

BUCKLING OF ECCENTRICALLY STIFFENED ORTHOTROPIC CYLINDERS UNDER PURE BENDING

by David L. Block

Langley Research Center
Langley Station, Hampton, Va.

NATIONAL AERONAUTICS AND SPACE ADMINISTRATION • WASHINGTON, D. C. • MARCH 1966

NASA TN D-3351

BUCKLING OF ECCENTRICALLY STIFFENED ORTHOTROPIC CYLINDERS UNDER PURE BENDING

By David L. Block

Langley Research Center
Langley Station, Hampton, Va.

NATIONAL AERONAUTICS AND SPACE ADMINISTRATION

For sale by the Clearinghouse for Federal Scientific and Technical Information
Springfield, Virginia 22151 – Price $0.30

BUCKLING OF ECCENTRICALLY STIFFENED ORTHOTROPIC CYLINDERS UNDER PURE BENDING

By David L. Block
Langley Research Center

SUMMARY

The stability of stiffened orthotropic cylinders which include the effects of eccentric stiffeners and are loaded with pure bending or any combination of bending and compression is investigated analytically by means of a small deflection theory. Solutions to the buckling equations are obtained for simple support boundary conditions by use of the Galerkin method. The pure bending buckling loads are compared with existing pure compression buckling loads for three contemporary cylinder configurations. Also shown are predicted buckling modes and typical interaction curves between bending and compression. The results show that eccentricity effects are substantial and that the maximum pure bending load may be as much as 40 percent greater than the pure compression load.

INTRODUCTION

The effect of eccentricity or one-sidedness of stiffening elements in determining buckling loads of stiffened cylinders has been shown to be of great importance. (See refs. 1 to 4.) In reference 3, a theory for eccentrically stiffened orthotropic cylinders employing Donnell-type assumptions and neglecting prebuckling deformations was derived from energy principles, and buckling solutions were obtained for a simply supported cylinder under any combination of uniform axial load and lateral pressure.

The purpose of this paper is to extend the analysis of reference 3 to include the buckling of an eccentrically stiffened orthotropic cylinder subject to a loading of pure bending or combination bending and compression (nonuniform axial loading). The equations developed are also valid for an unstiffened cylindrical orthotropic shell. Solutions to the buckling equations corresponding to classical simple support boundary conditions are obtained by use of the Galerkin method in a manner similar to that employed in reference 5 in which an unstiffened isotropic cylinder under pure bending was investigated. Maximum compressive stress resultant at buckling due to bending, hereafter referred to as maximum bending loads, are compared with uniform compression loads for three types of cylinders with contemporary geometry, that is, ring-stiffened corrugated cylinders, ring- and stringer-stiffened isotropic cylinders, and longitudinally stiffened

isotropic cylinders. Interaction curves between bending and compression and the buckling mode shapes are also presented.

SYMBOLS

The units used for the physical quantities in this report are given both in the U.S. Customary Units and in the International System of Units (SI). The relationship between these two systems of units can be found in reference 6.

A	cross-sectional area of stiffener
a	length of stiffened cylinder (see fig. 1)
a_n,b_n,c_n	constant coefficients of deflection functions
D_x,D_y	bending stiffnesses of orthotropic plate in longitudinal and circumferential directions, respectively
D_{xy}	twisting stiffness of orthotropic plate
d	stringer spacing (see fig. 1)
E	Young's modulus
E_x,E_y	extensional stiffnesses of orthotropic plate in longitudinal and circumferential directions, respectively
G	shear modulus
G_{xy}	inplane shear stiffness of orthotropic plate
I_o	moment of inertia of stiffener about middle surface of shell
i,j,n,q,p	integers
J	torsional constant for stiffener
l	ring spacing (see fig. 1)
m	number of half waves in cylinder buckle pattern in longitudinal direction
N_x	total compressive stress resultant
N_{x_b}	maximum compressive stress resultant due to bending
$\bar{N}_{x_b}$	critical maximum compressive stress resultant due to bending when $N_{x_c} = 0$

N_{x_c} uniform compressive stress resultant

$\bar{N}_{x_c}$ critical compressive stress resultant when $N_{x_b} = 0$

R radius of cylinder to middle surface of shell (see fig. 1)

t thickness of isotropic cylindrical shell wall

$\bar{t}$ effective wall thickness of stiffened isotropic cylinder, $\frac{A_s}{d} + t$

u,v,w displacements in x-, y-, and z-directions, respectively, of a point in middle surface of shell

x,y,z orthogonal curvilinear coordinates with origin lying in middle surface of shell (see fig. 1)

$\bar{z}$ distance from centroid of stiffener to middle surface of shell (see fig. 1), positive if stiffener lies on external surface of shell and negative if stiffener lies on internal surface

δ_{ij} Kronecker delta, $\delta_{ij} = 0$ when $i \neq j$ and $\delta_{ij} = 1$ when $i = j$

μ_x, μ_y Poisson's ratios for bending of orthotropic plate in longitudinal and circumferential directions, respectively

μ_x', μ_y' Poisson's ratios for extension of orthotropic plate in longitudinal and circumferential directions, respectively

Subscripts:

s,r stringers (longitudinal stiffening, parallel to x-axis) and rings (transverse stiffening, parallel to y-axis), respectively

x,y longitudinal and circumferential directions, respectively

A subscript preceded by a comma denotes partial differentiation with respect to the subscript.

THEORETICAL SOLUTION

The equations of equilibrium governing the buckling of a stiffened cylinder subject to inplane axial stresses only are (ref. 3):

$$\frac{E_x}{1 - \mu_x'\mu_y'} u_{,xx} + \frac{E_s A_s}{d}\left(u_{,xx} - \bar{z}_s w_{,xxx}\right) + \frac{\mu_y' E_x}{1 - \mu_x'\mu_y'}\left(v_{,xy} + \frac{w_{,x}}{R}\right) + G_{xy}\left(u_{,yy} + v_{,xy}\right) = 0 \tag{1a}$$

$$\frac{E_y}{1 - \mu_x'\mu_y'}\left(v_{,yy} + \frac{w_{,y}}{R}\right) + \frac{E_rA_r}{l}\left(v_{,yy} + \frac{w_{,y}}{R} - \bar{z}_r w_{,yyy}\right)$$

$$+ \frac{\mu_x' E_y}{1 - \mu_x'\mu_y'} u_{,xy} + G_{xy}\left(u_{,xy} + v_{,xx}\right) = 0 \tag{1b}$$

$$\left(\frac{D_x}{1 - \mu_x\mu_y} + \frac{E_sI_{o_s}}{d}\right) w_{,xxxx} + \left(\frac{\mu_y D_x}{1 - \mu_x\mu_y} + 2D_{xy} + \frac{\mu_x D_y}{1 - \mu_x\mu_y} + \frac{G_sJ_s}{d} + \frac{G_rJ_r}{l}\right) w_{,xxyy}$$

$$+ \left(\frac{D_y}{1 - \mu_x\mu_y} + \frac{E_rI_{o_r}}{l}\right) w_{,yyyy} + \frac{E_y}{R\left(1 - \mu_x'\mu_y'\right)}\left(\mu_x' u_{,x} + v_{,y} + \frac{w}{R}\right)$$

$$- \frac{E_sA_s}{d}\bar{z}_s u_{,xxx} - \frac{E_rA_r}{l}\bar{z}_r\left(\frac{2w_{,yy}}{R} + v_{,yyy}\right) + \frac{E_rA_r}{Rl}\left(v_{,y} + \frac{w}{R}\right) + N_x w_{,xx} = 0 \tag{1c}$$

When equations (1) for a stiffened cylinder (fig. 1) were developed, the following basic assumptions were made. The stiffened cylinder is composed of an orthotropic shell with infinite transverse shear stiffnesses and with elastic constants as given in reference 7. The stiffening elements are uniform equally spaced rings and stringers which are assumed to have elastic properties and to be closely spaced so that their elastic properties can be averaged over the stiffener spacing. The usual Donnell-type assumptions are used to specify buckling displacements in the shell. The stiffeners are treated as beam elements with stiffener twisting accounted for in an approximate manner. In cases where both rings and stringers lie on the same surface of the shell, the effect of joints in the stiffening framework is ignored.

The cylinder loading is taken to be a combination of bending and compression, in which the inplane loading prior to buckling is given by

$$N_x = N_{x_c} + N_{x_b} \cos\frac{y}{R} \tag{2}$$

where N_{x_c} is the uniform compressive stress resultant and N_{x_b} is the maximum bending stress resultant; both are positive in compression.

The boundary conditions to be satisfied are those of simple support which are given in reference 3 as

$$w = 0$$

$$\frac{D_x}{1 - \mu_x\mu_y}\left(w_{,xx} + \mu_y w_{,yy}\right) + \frac{E_S I_{O_S}}{d} w_{,xx} - \frac{E_S A_S}{d}\bar{z}_S u_{,x} = 0$$

$$\frac{E_x}{1 - \mu_x'\mu_y'}\left[u_{,x} + \mu_y'\left(v_{,y} + \frac{w}{R}\right)\right] + \frac{E_S A_S}{d} u_{,x} - \frac{E_S A_S}{d}\bar{z}_S w_{,xx} = 0$$

$$v = 0$$

Expressions for the displacements which satisfy these boundary conditions are:

$$\left.\begin{aligned} u &= \cos\frac{m\pi x}{a}\sum_{n=0}^{\infty} c_n \cos\frac{ny}{R} \\ v &= \sin\frac{m\pi x}{a}\sum_{n=0}^{\infty} b_n \sin\frac{ny}{R} \\ w &= \sin\frac{m\pi x}{a}\sum_{n=0}^{\infty} a_n \cos\frac{ny}{R} \end{aligned}\right\} \qquad (3)$$

where m denotes the number of axial half waves in the buckle pattern.

By substituting equations (3) into equations (1a) and (1b), the coefficients b_n and c_n may be determined as functions of the coefficients a_n and from equations (1c), (2), and (3) the following equation is obtained:

$$Q(w) = \sum_{n=0}^{\infty} a_n\left[A_{33} + A_{23}\left(\frac{A_{12}A_{13} - A_{11}A_{23}}{A_{11}A_{22} - A_{12}^2}\right) + A_{13}\left(\frac{A_{12}A_{23} - A_{13}A_{22}}{A_{11}A_{22} - A_{12}^2}\right)\right.$$
$$\left. - \left(N_{x_c} + N_{x_b}\cos\frac{y}{R}\right)\left(\frac{m\pi}{a}\right)^2\right]\sin\frac{m\pi x}{a}\cos\frac{ny}{R} = 0 \qquad (4)$$

in which

$$A_{11} = \left(\frac{E_x}{1 - \mu_x'\mu_y'} + \frac{E_S A_S}{d}\right)\left(\frac{m\pi}{a}\right)^2 + G_{xy}\left(\frac{n}{R}\right)^2$$

$$A_{12} = \left(\frac{\mu_y' E_x}{1 - \mu_x' \mu_y'} + G_{xy}\right)\left(\frac{m\pi}{a}\right)\left(\frac{n}{R}\right)$$

$$A_{13} = \frac{1}{R}\left(\frac{\mu_y' E_x}{1 - \mu_x' \mu_y'}\right)\left(\frac{m\pi}{a}\right) + \frac{E_s A_s}{d}\bar{z}_s\left(\frac{m\pi}{a}\right)^3$$

$$A_{22} = G_{xy}\left(\frac{m\pi}{a}\right)^2 + \left(\frac{E_y}{1 - \mu_x' \mu_y'} + \frac{E_r A_r}{l}\right)\left(\frac{n}{R}\right)^2$$

$$A_{23} = \frac{1}{R}\left(\frac{E_y}{1 - \mu_x' \mu_y'} + \frac{E_r A_r}{l}\right)\left(\frac{n}{R}\right) + \frac{E_r A_r}{l}\bar{z}_r\left(\frac{n}{R}\right)^3$$

$$A_{33} = \left(\frac{D_x}{1 - \mu_x \mu_y} + \frac{E_s I_{o_s}}{d}\right)\left(\frac{m\pi}{a}\right)^4 + \left(\frac{2\mu_y D_x}{1 - \mu_x \mu_y} + 2D_{xy} + \frac{G_s J_s}{d} + \frac{G_r J_r}{l}\right)\left(\frac{m\pi}{a}\right)^2\left(\frac{n}{R}\right)^2$$

$$+ \left(\frac{D_y}{1 - \mu_x \mu_y} + \frac{E_r I_{o_r}}{l}\right)\left(\frac{n}{R}\right)^4 + \frac{1}{R^2}\left(\frac{E_y}{1 - \mu_x' \mu_y'} + \frac{E_r A_r}{l}\right) + 2\frac{E_r A_r}{l}\bar{z}_r\frac{n^2}{R^3}$$

where the reciprocal relations $\mu_x' E_y = \mu_y' E_x$ and $\mu_x D_y = \mu_y D_x$ (ref. 7) have been employed to simplify the equation.

By use of the Galerkin method, a set of equations for the unknown coefficients a_n is then

$$\int_0^a \int_0^{2\pi R} Q(w) \sin\frac{p\pi x}{a} \cos\frac{qy}{R}\, dx\, dy = 0 \tag{5}$$

from which a homogeneous set of equations is determined as

$$a_n\left(F_n - N_{x_c}\right) - \frac{N_{x_b}}{2}\left[\left(1 + \delta_{1n} - \delta_{0n}\right)a_{n-1} + a_{n+1}\right] = 0 \tag{6}$$

where

$$F_n = \left(\frac{a}{m\pi}\right)^2\left[A_{33} + A_{23}\left(\frac{A_{12}A_{13} - A_{11}A_{23}}{A_{11}A_{22} - A_{12}^2}\right) + A_{13}\left(\frac{A_{12}A_{23} - A_{13}A_{22}}{A_{11}A_{22} - A_{12}^2}\right)\right]$$

$$n = 0, 1, 2, 3, \ldots$$

$$\delta_{jn} = 1 \qquad (j = n)$$

$$\delta_{jn} = 0 \qquad (j \neq n)$$

Equation (6) can be used to determine buckling loads under pure bending and pure compression (where the equation reduces to the result given in ref. 3) and to investigate interactions between bending and compression. For nontrivial solutions of equation (6), the determinant of the coefficients must equal zero. When computing the buckling load for a specified loading, the determinant is minimized numerically for integral values of m, the number of axial half waves in the buckle pattern. The size of the determinant is determined by requiring that the buckling load converges to a desired accuracy. For the calculations presented herein, the size of the determinant was increased until the buckling load between a specified order determinant and a determinant of one less order did not vary by more than 0.5 percent. All the numerical calculations presented herein were performed on an electronic computer.

RESULTS AND DISCUSSION

Because of the large number of geometric parameters involved in equation (6), it is impractical to present results of a general nature. However, it is of value to present some computed results for cylinders of contemporary proportions in order to study loadings of pure bending compared with pure compression, eccentricity effects under these loadings, and interaction between bending and compression. Therefore, computations of bending loads were made for three types of stiffened cylinders appropriate for large-diameter booster interstage structures: ring-stiffened corrugated cylinders, ring- and stringer-stiffened isotropic cylinders, and longitudinally (stringer) stiffened isotropic cylinders. For the calculations, the material in the cylindrical shell and the material in the stiffeners were taken to be identical, and a value of 0.32 was assigned to Poisson's ratio for the stiffened isotropic shells. The dimensions of the cylinders are given in figure 2. Eccentricity effects for each cylinder configuration were studied by moving the stiffeners from the internal to the external surface of the shell.

The results of the computations are presented in table I and in figures 3 to 9. Details and discussion of the computed results for each cylinder configuration follow.

The maximum pure bending loads for general instability failure of ring-stiffened corrugated cylinders and for general and panel instability failure of ring- and stringer-stiffened cylinders are presented in table I and are shown in figures 3, 4, and 5, respectively. In the figures, a nondimensional buckling load parameter $\overline{N}_{x_b}/E_x$ or $\overline{N}_{x_c}/E_x$

for corrugated cylinders and $\overline{N}_{x_b}/E\bar{t}$ or $\overline{N}_{x_c}/E\bar{t}$ for ring- and stringer-stiffened cylinders, is plotted against a nondimensional ring spacing l/R. For the panel instability calculations, the ring spacing l was taken to be the length of the cylinder, and thus the cylinder is a longitudinally (stringer) stiffened isotropic cylinder. Results are presented for cylinders loaded in pure bending (computed by using eq. (6)) or loaded in pure compression (computed by using eq. (15) or (17) of ref. 3).

For the ring-stiffened corrugated cylinders studied, the computed results (table I(a) and fig. 3) indicate that eccentricity effects are as important for pure bending loads as those observed for pure compression (ref. 3). For internally stiffened cylinders, the critical maximum bending load was found to be as much as 40 percent greater than the critical pure compression load. (See last column of table I(a).) This percentage increase is somewhat greater than similar results of 25 percent presented in reference 4; however, the corrugated cylinders in reference 4 do not have the same properties as the ones examined herein and, therefore, the two results would not be expected to agree.

For the ring- and stringer-stiffened and the longitudinally stiffened isotropic cylinders, the computed results (tables I(b) and I(c) and figs. 4 and 5) show that the differences between external and internal stiffeners are not as large as those observed for the corrugated cylinders, but nevertheless, both effects may be substantial and must be considered.

In figures 6 and 7, typical interaction curves between bending and compression are shown for the corrugated cylinder and for the ring- and stringer-stiffened cylinder, respectively. The interaction curve for the internally stiffened corrugated cylinder possesses a vertical tangent at the abscissa as observed in reference 4; however, for the other interaction curves this behavior was not as pronounced. Hence, except for the internally stiffened corrugated cylinder, the interaction curves presented may be approximated by straight lines.

In figures 8 and 9, the buckling mode shapes for pure bending and pure compression are shown (corresponding to the end points of the interaction curves of figs. 6 and 7). The buckle shapes for pure bending show that the buckles are localized on the compression area of the cylinder, a result observed in references 4 and 5.

In addition to these cylinder configurations, calculations were made for unstiffened isotropic and orthotropic cylinders by setting the ring and stringer properties equal to zero and using the appropriate cylindrical shell constants in equation (6). For isotropic cylinders, the calculations showed that the effects of bending are negligible when compared with compression which agreed with references 5 and 8. The three cylinder configurations considered herein were analyzed as orthotropic shells by using orthotropic constants defined in reference 3. The calculations for these cylinders showed that even though eccentricity effects are neglected, there can be a considerable increase in the critical

compression load due to bending; for example, the corrugated cylinder gave an increase of 18 percent.

Additional information can be obtained by considering the circumferential buckling modes for pure compression which are given in reference 3. The results presented in table I indicate generally that the differences between pure bending and pure compression loads may be considered small when the cylinder has an axisymmetric pure compressive buckling mode (for example, externally stiffened corrugated cylinders or unstiffened isotropic cylinders) or when the cylinder has a pure compressive buckling mode with a large number of circumferential waves (longitudinally stiffened cylinders). However, the results indicate large differences between bending and compression for cylinders which have pure compressive modes consisting of intermediate numbers (for example, 6 to 15) of circumferential waves, such as the internally stiffened corrugated cylinders or the ring- and stringer-stiffened isotropic cylinders.

Also from table I it may be noted that the size of the determinant needed for convergence will depend upon the number of waves in the circumferential pure compressive buckling mode; that is, cylinders buckling with a small number of circumferential waves in compression will require fewer terms to approximate the buckle shape in bending and a smaller determinant order will be required for convergence of the buckling load.

CONCLUDING REMARKS

A stability equation for eccentrically stiffened orthotropic cylinders subject to a loading of pure bending or to combination bending and compression has been derived by means of the Galerkin method for simple support boundary conditions. Sample calculations have been shown for three types of contemporary stiffened cylinders to illustrate the importance of bending loads, eccentricity effects under these loads, and interaction between bending and compression. The calculations presented show that the difference in predicted buckling load between a cylinder loaded in pure bending or pure compression may be considered small when the pure compressive buckling mode is axisymmetric or has a large number of circumferential waves. The buckling analysis of cylinders, which buckle in compressive buckling modes with a moderate number of circumferential waves and which are to be loaded in bending, require the use of an analysis which accounts for the bending load. The calculations also show substantial eccentricity effects in bending comparable with those obtained for cylinders in compression.

Langley Research Center,
National Aeronautics and Space Administration,
Langley Station, Hampton, Va., January 14, 1966.

REFERENCES

1. Van der Neut, A.: The General Instability of Stiffened Cylindrical Shells Under Axial Compression. Rept. S. 314, Natl. Aeron. Res. Inst. (Amsterdam), 1947.

2. Baruch, M.; and Singer, J.: Effect of Eccentricity of Stiffeners on the General Instability of Stiffened Cylindrical Shells Under Hydrostatic Pressure. J. Mech. Eng. Sci., vol. 5, no. 1, 1963, pp. 23-27.

3. Block, David L.; Card, Michael F.; and Mikulas, Martin M., Jr.: Buckling of Eccentrically Stiffened Orthotropic Cylinders. NASA TN D-2960, 1965.

4. Hedgepeth, John M.; and Hall, David B.: Stability of Stiffened Cylinders. Paper No. 65-79, Am. Inst. Aeron. Astronaut., Jan. 1965.

5. Seide, Paul; and Weingarten, V. I.: On the Buckling of Circular Cylindrical Shells Under Pure Bending. Trans. ASME, Ser. E: J. Appl. Mech., vol. 28, no. 1, Mar. 1961, pp. 112-116.

6. Mechtly, E. A.: The International System of Units – Physical Constants and Conversion Factors. NASA SP-7012, 1964.

7. Stein, Manuel; and Mayers, J.: A Small-Deflection Theory for Curved Sandwich Plates. NACA Rept. 1008, 1951. (Supersedes NACA TN 2017.)

8. Bijlaard, P. P.; and Gallagher, R. H.: Elastic Instability of a Cylindrical Shell Under Arbitrary Circumferential Variation of Axial Stress. J. Aerospace Sci., vol. 27, no. 11, Nov. 1960, pp. 854-858, 866.

TABLE I.- BUCKLING CALCULATIONS FOR STIFFENED CYLINDERS

(a) Ring-stiffened corrugated cylinders

l/R	$\bar{N}_{x_b}/E_x$	m	Minimum determinant*	$\bar{N}_{x_b}/\bar{N}_{x_c}$
Rings, external				
0.15	0.005514	2	6	1.089
.20	.004679	2	6	1.091
.25	.004171	2	6	1.090
.30	.003828	2	6	1.088
.35	.003581	2	6	1.086
.40	.003391	2	7	1.083
.45	.003245	2	7	1.080
.50	.003128	2	7	1.079
Rings, internal				
0.15	0.002458	1	10	1.396
.20	.002084	1	10	1.397
.25	.001839	1	11	1.389
.30	.001666	1	11	1.376
.35	.001536	1	11	1.376
.40	.001442	1	11	1.352
.45	.001353	1	11	1.341
.50	.001286	1	11	1.329

(b) Ring- and stringer-stiffened cylinders

l/R	$\bar{N}_{x_b}/E\bar{t}$	m	Minimum determinant*	$\bar{N}_{x_b}/\bar{N}_{x_c}$
Stringers, external; rings, external				
0.05	0.006239	5	10	1.045
.10	.005318	4	12	1.038
.15	.004972	4	12	1.050
.20	.004788	4	12	1.072
.25	.004666	3	14	1.089
Stringers, external; rings, internal				
0.05	0.004752	4	14	1.156
.10	.004335	3	14	1.130
.15	.004144	3	14	1.114
.20	.004025	3	16	1.109
.25	.003938	3	16	1.101
Stringers, internal; rings, internal				
0.05	0.004470	3	14	1.187
.10	.003949	3	14	1.151
.15	.003669	3	14	1.159
.20	.003476	3	16	1.163
.25	.003319	2	16	1.194

(c) Longitudinally stiffened cylinders

l/R	$\bar{N}_{x_b}/E\bar{t}$	m	Minimum determinant*	$\bar{N}_{x_b}/\bar{N}_{x_c}$
Stiffeners, external				
0.15	0.007133	1	12	1.013
.20	.004810	1	12	1.015
.25	.003681	1	26	1.019
.30	.002866	1	32	1.018
.35	.002291	1	34	1.022
.40	.001883	1	36	1.022
.45	.001596	1	34	1.027
.50	.001379	1	34	1.029
Stiffeners, internal				
0.15	0.006888	1	30	1.021
.20	.003909	1	28	1.027
.25	.002522	1	28	1.032
.30	.001769	1	28	1.037
.35	.001315	1	28	1.047
.40	.001022	1	26	1.048
.45	.000821	1	26	1.053
.50	.000679	1	26	1.058

*Minimum order of determinants required for 0.5-percent error in buckling load.

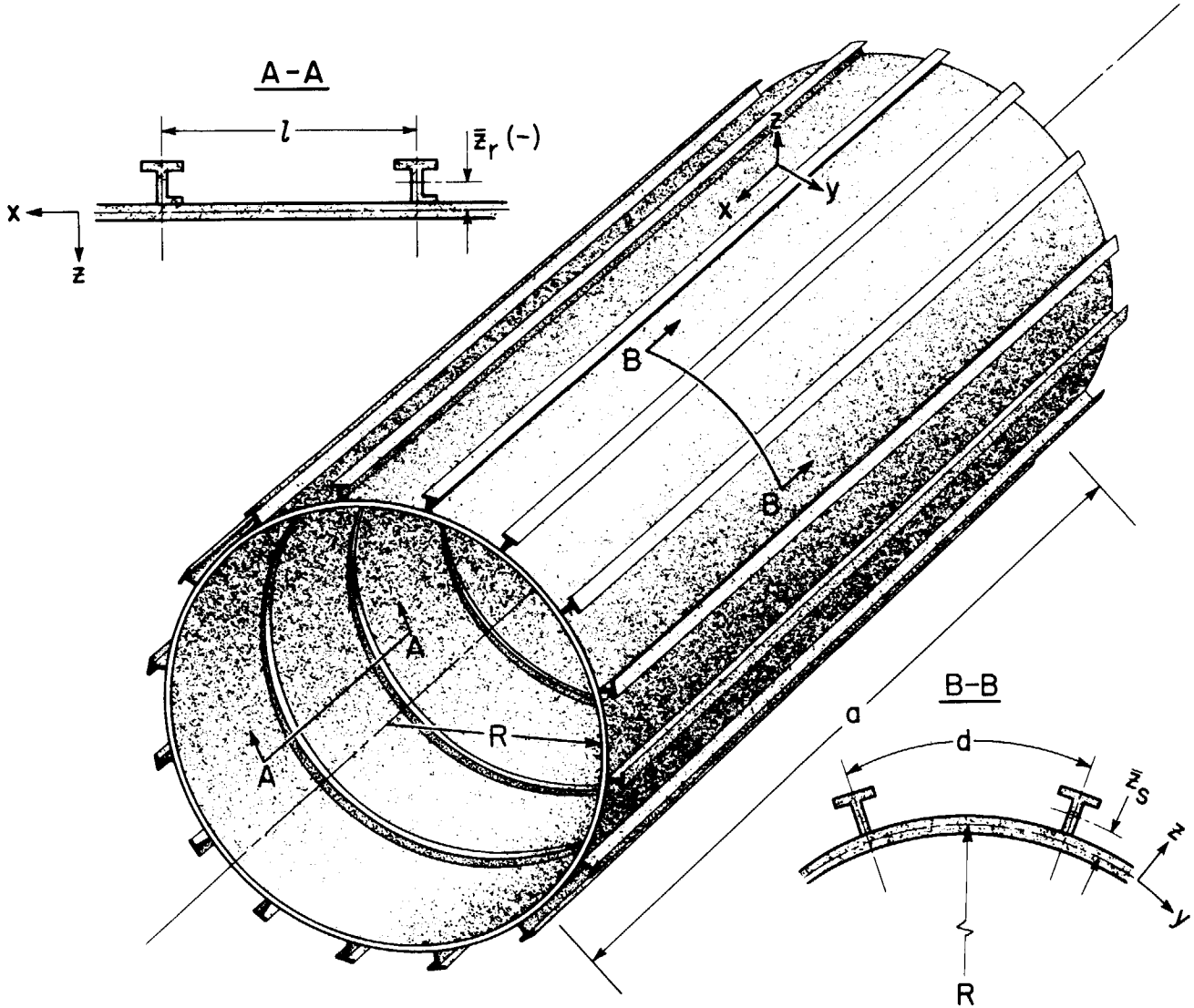

Figure 1.- Geometry of eccentrically stiffened cylinder.

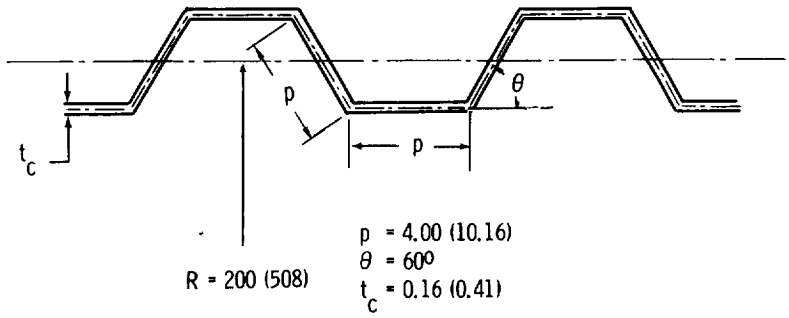

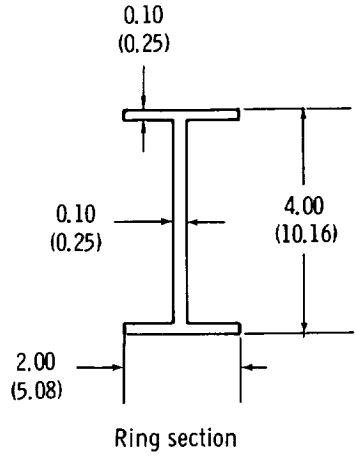

(a) Ring-stiffened corrugated cylinders; a = 200 in. (508 cm).

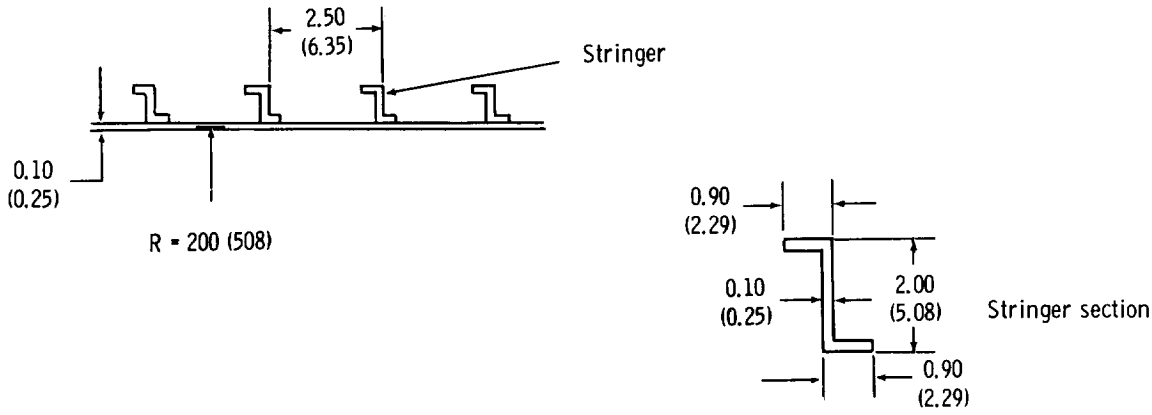

(b) Ring- and stringer-stiffened cylinders; a = 200 in. (508 cm). (See fig. 2(a) for ring section.)

Figure 2.- Dimensions of stiffened cylinder walls. Dimensions are in inches. (Parenthetical dimensions in cm.)

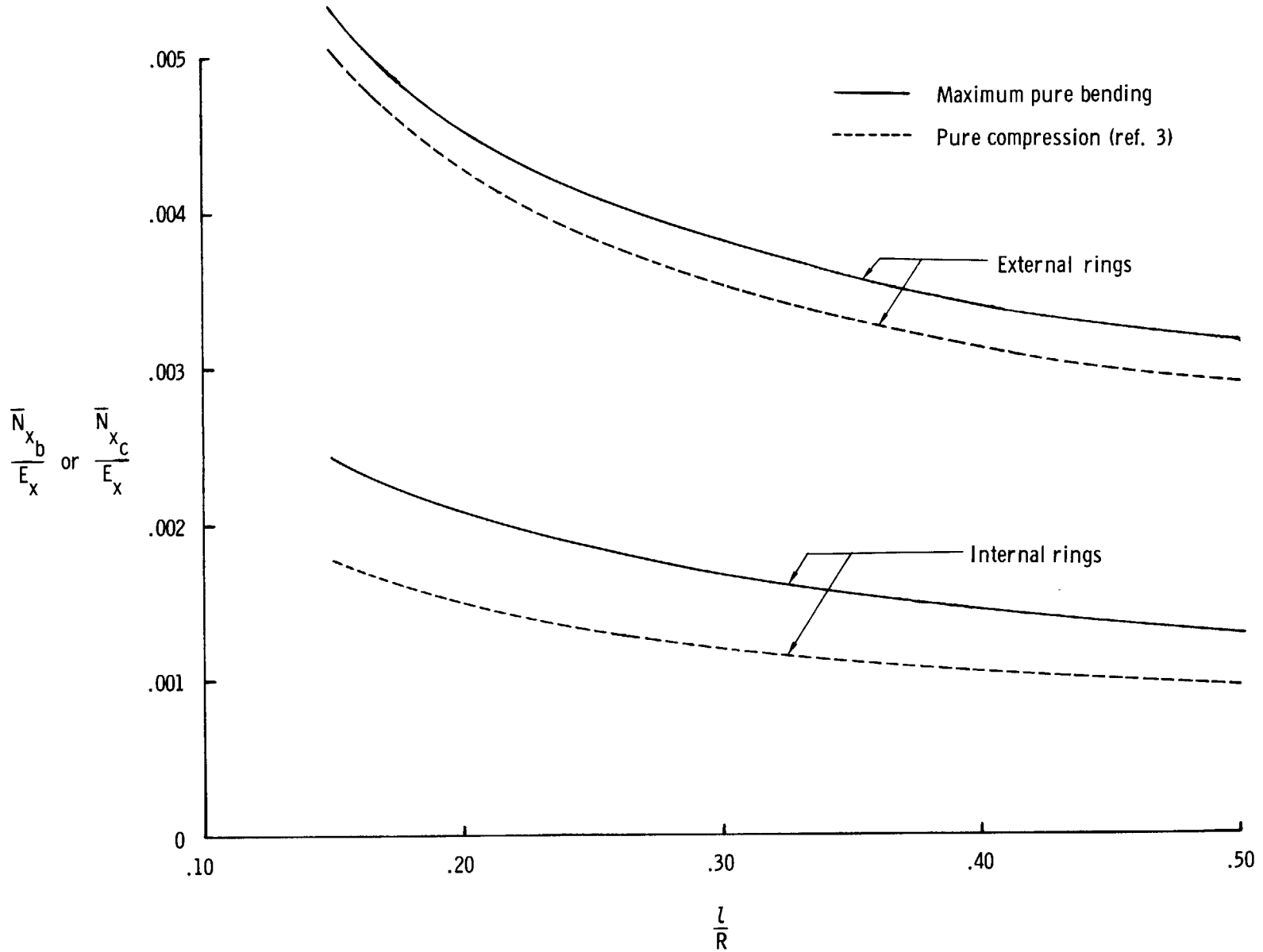

Figure 3.- General instability predictions for ring-stiffened corrugated cylinders.

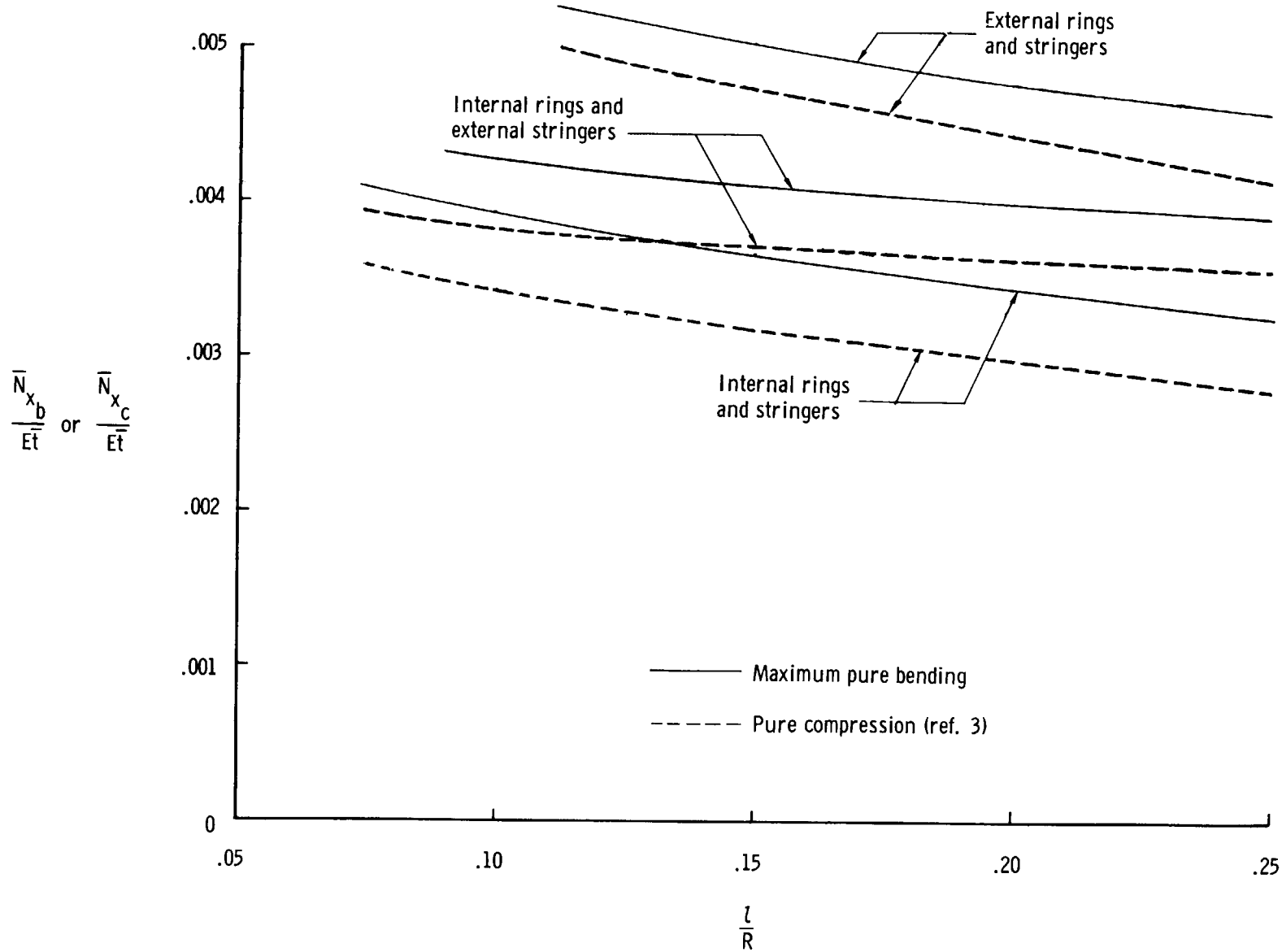

Figure 4.- General instability predictions for ring- and stringer-stiffened cylinders.

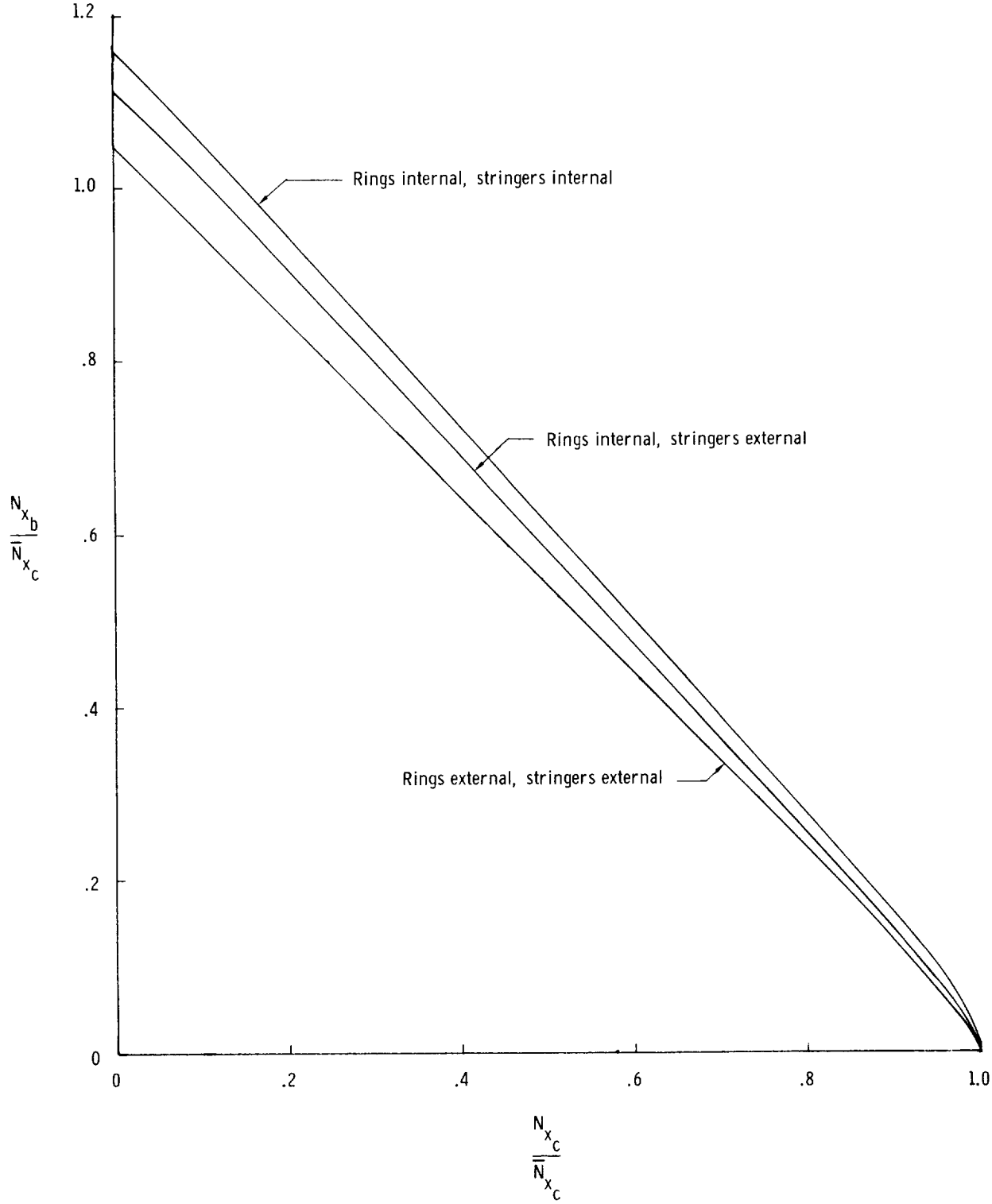

Figure 7.- Interaction curve for ring- and stringer-stiffened cylinder with $l/R = 0.15$.

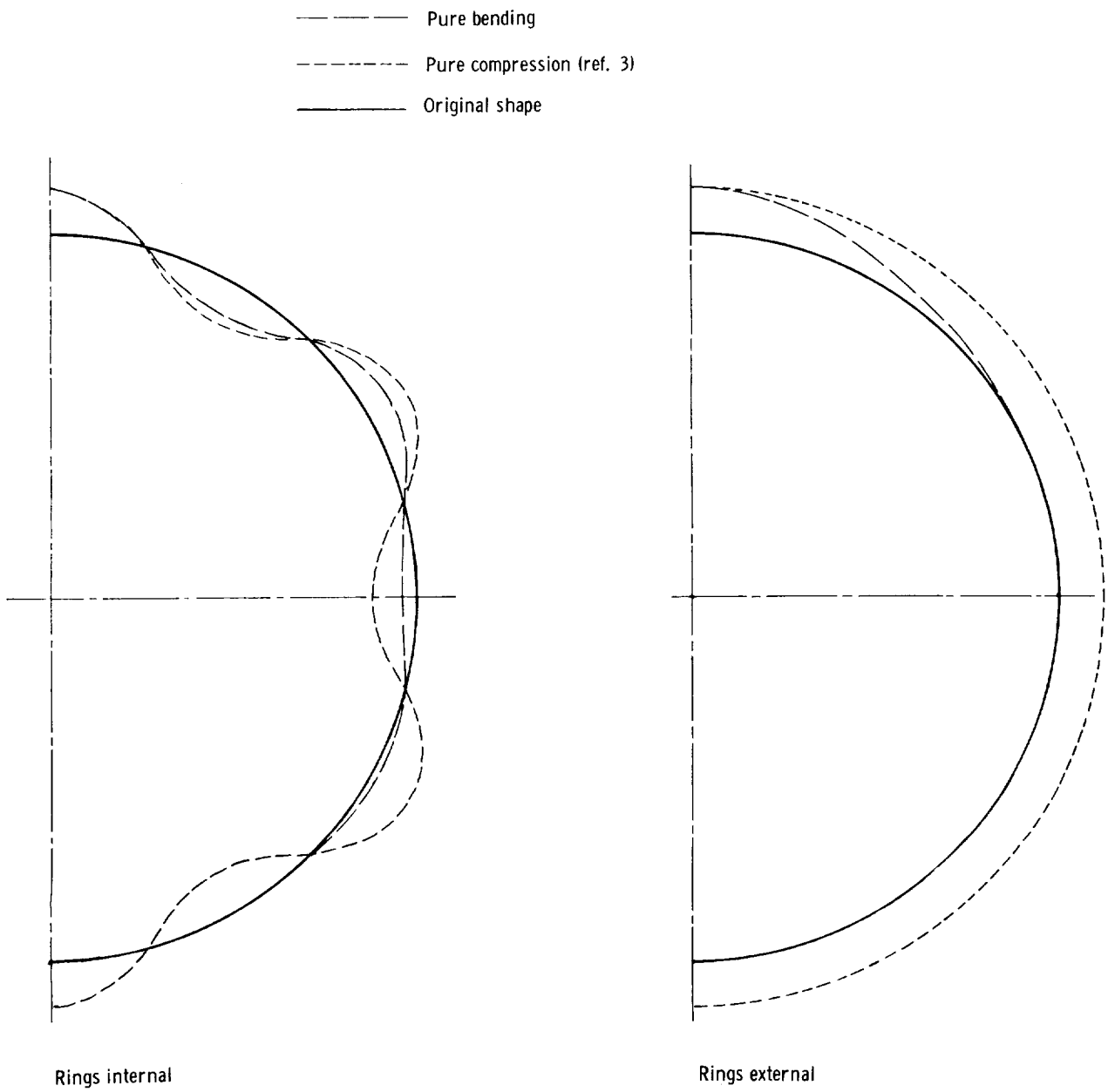

Figure 8.- Predicted mode shapes for ring-stiffened corrugated cylinder with $t/R = 0.2$.

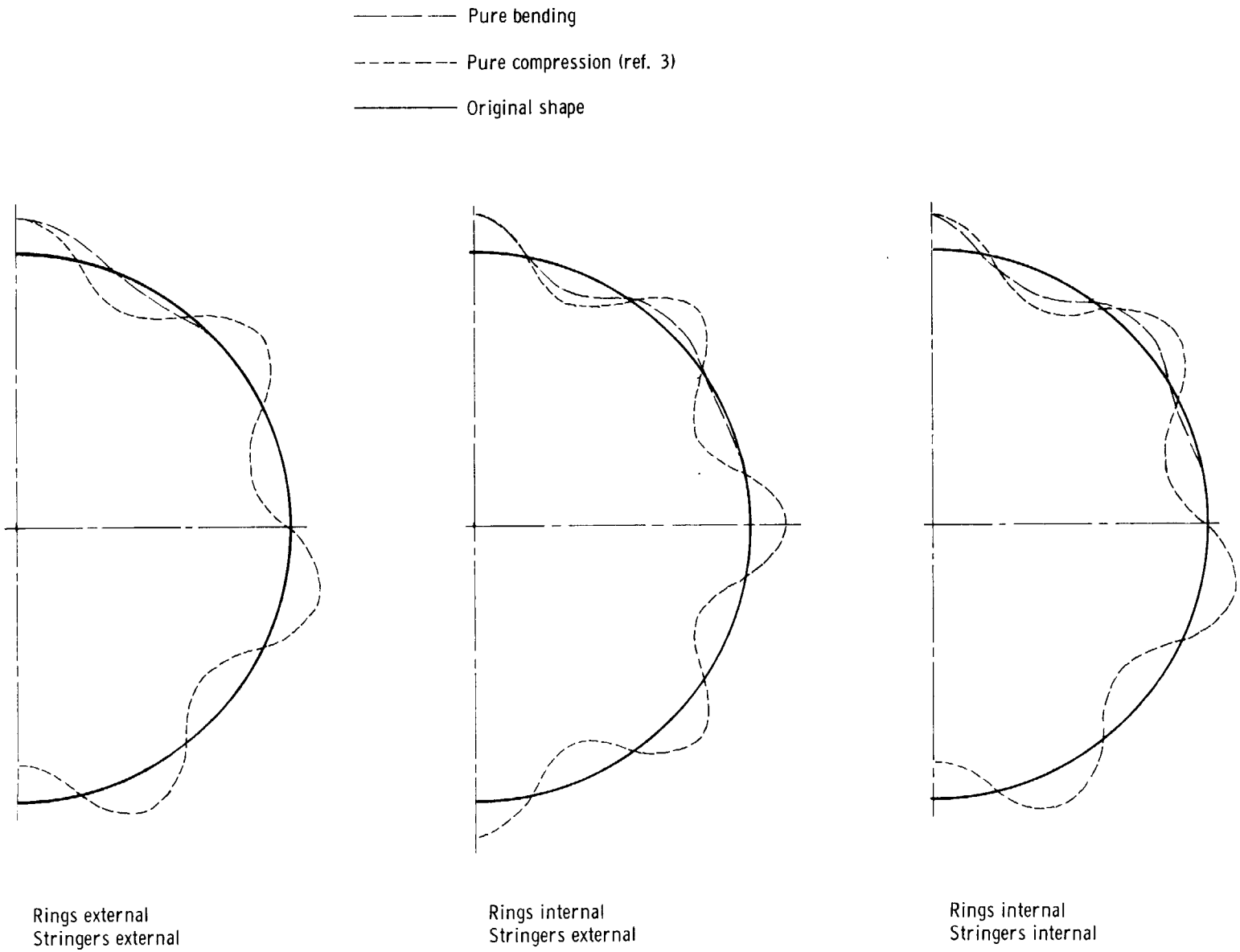

Figure 9.- Predicted mode shapes for ring- and stringer-stiffened cylinder with $l/R = 0.15$.

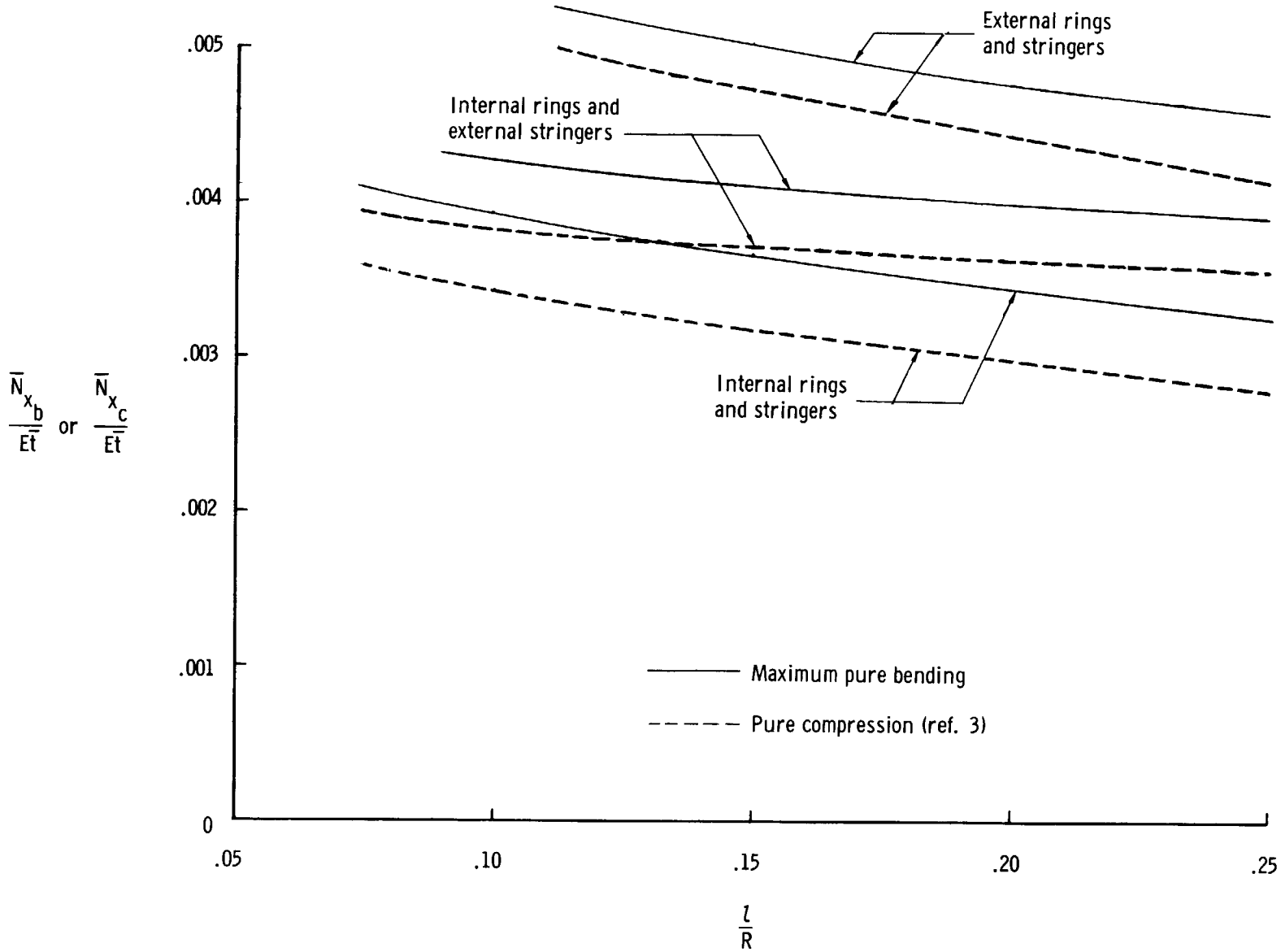

Figure 4.- General instability predictions for ring- and stringer-stiffened cylinders.

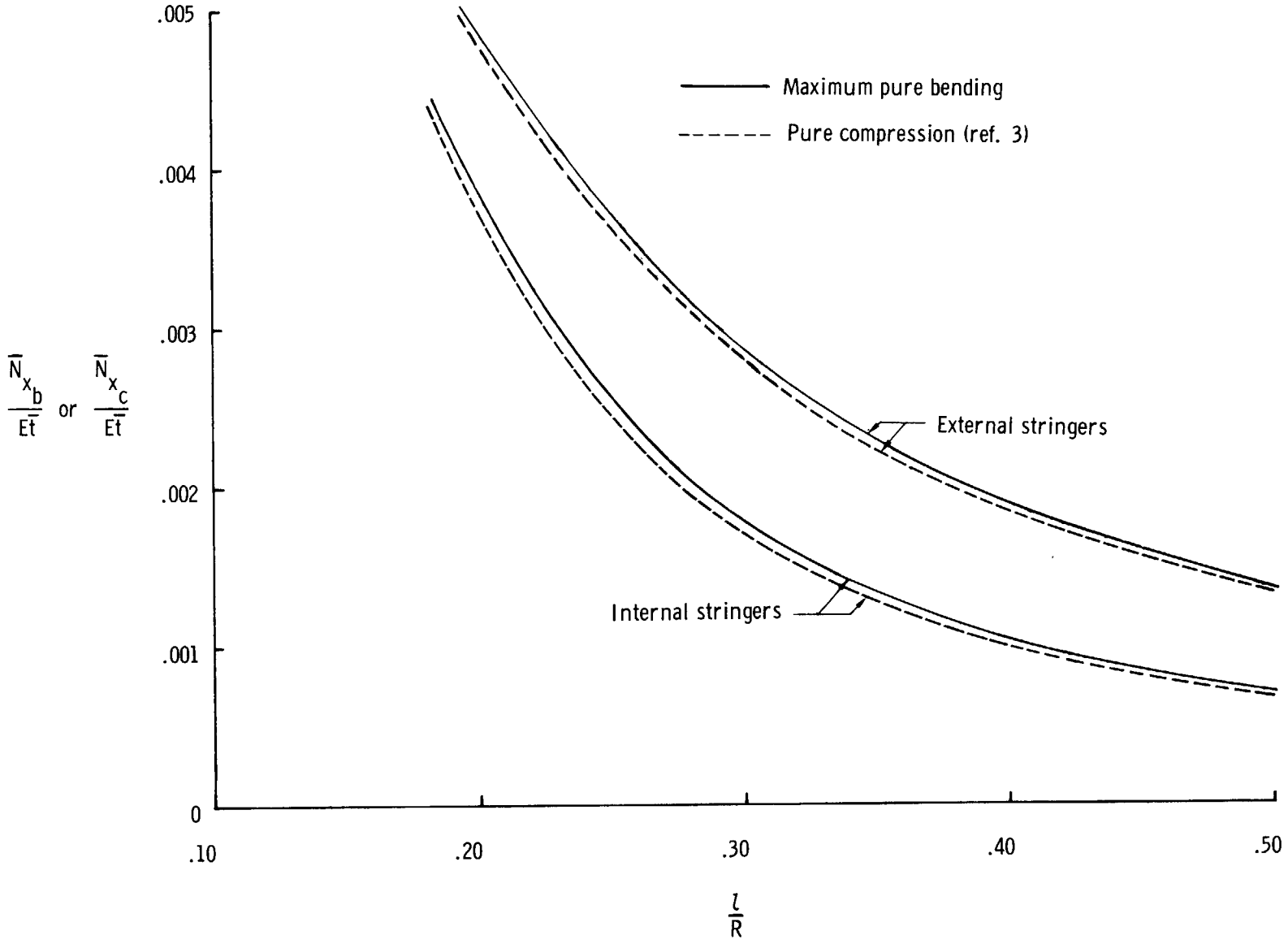

Figure 5.- Panel instability predictions for longitudinally stiffened cylinders.

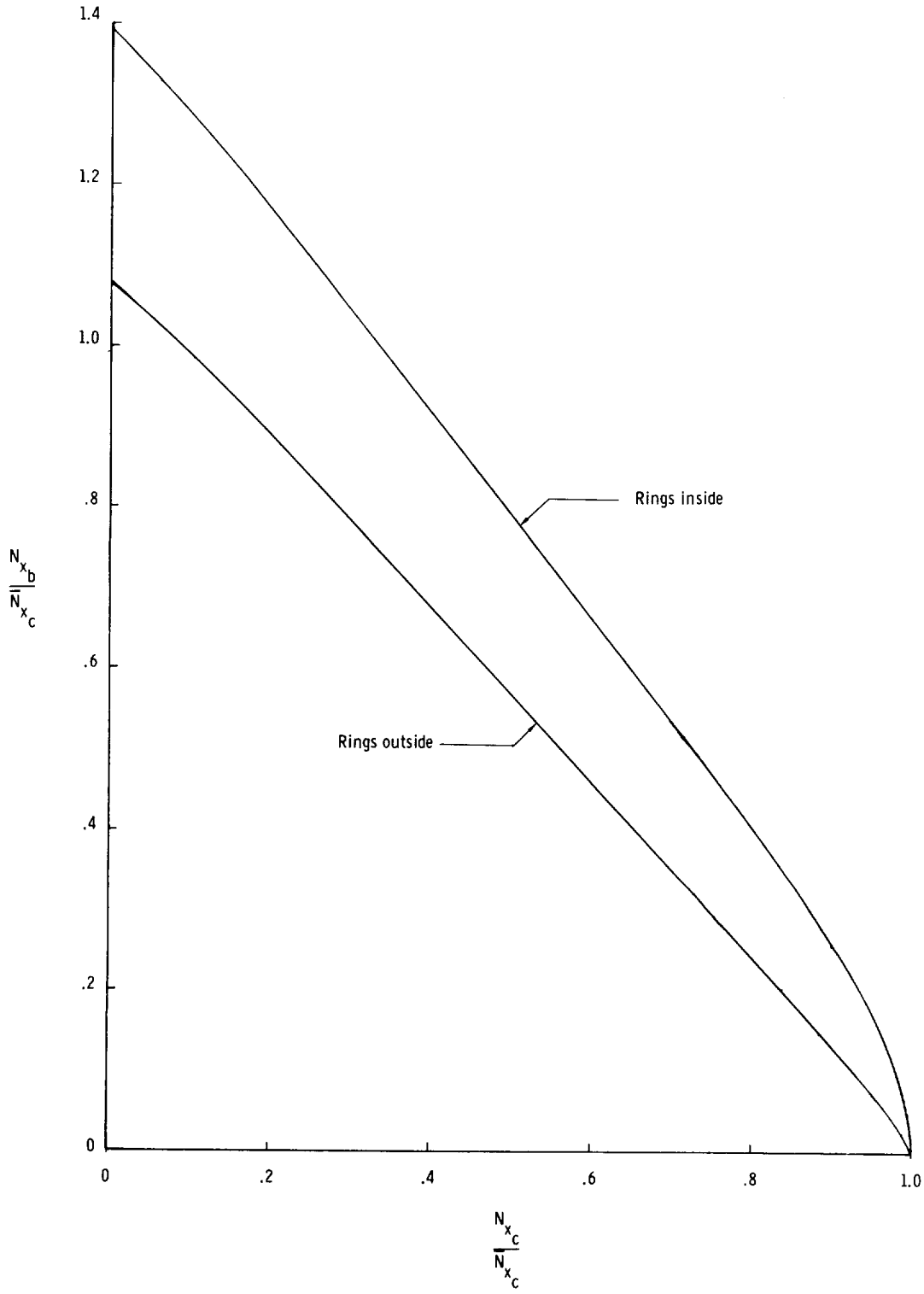

Figure 6.- Interaction curve for ring-stiffened corrugated cylinder with $l/R = 0.2$.

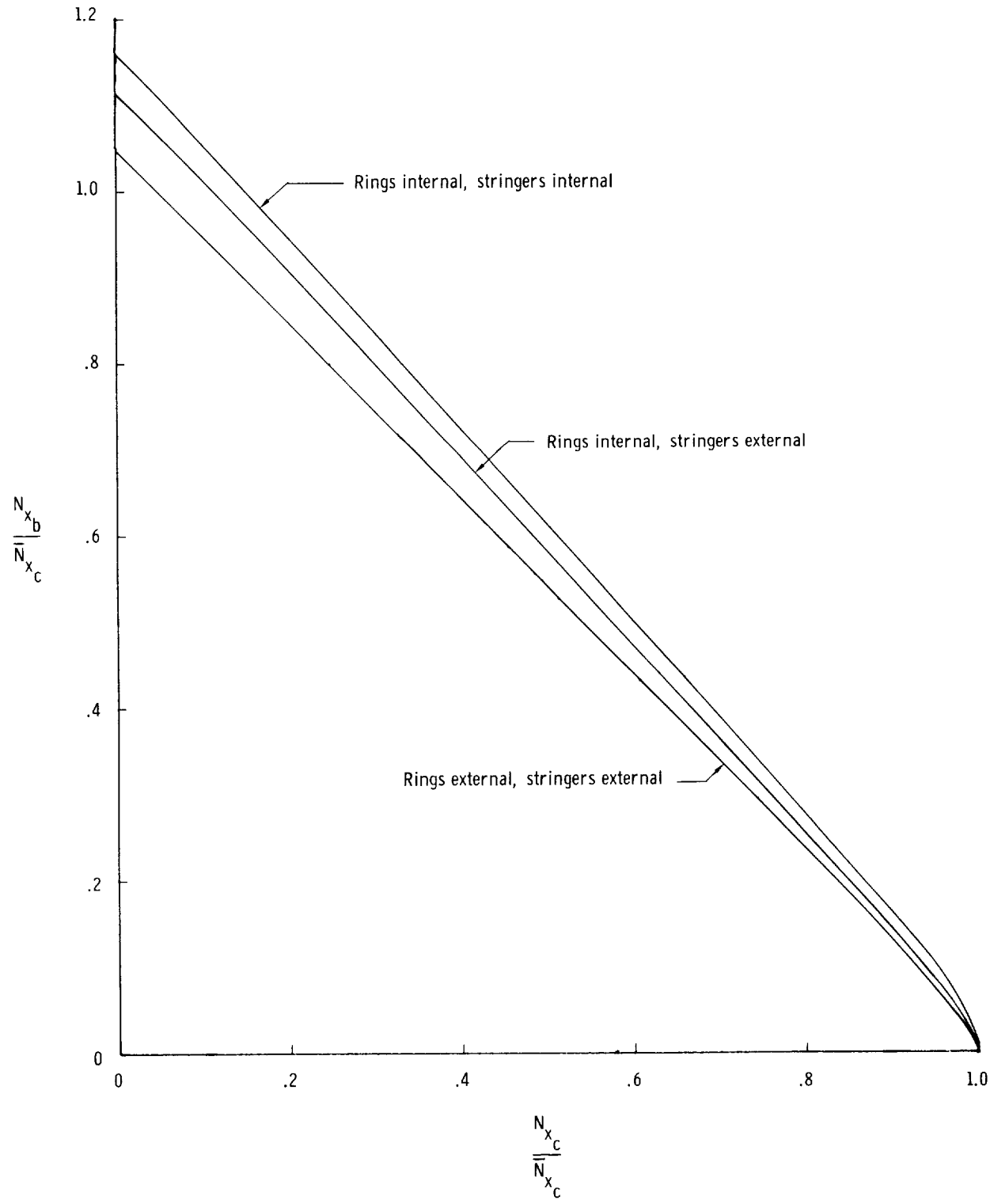

Figure 7.- Interaction curve for ring- and stringer-stiffened cylinder with $l/R = 0.15$.

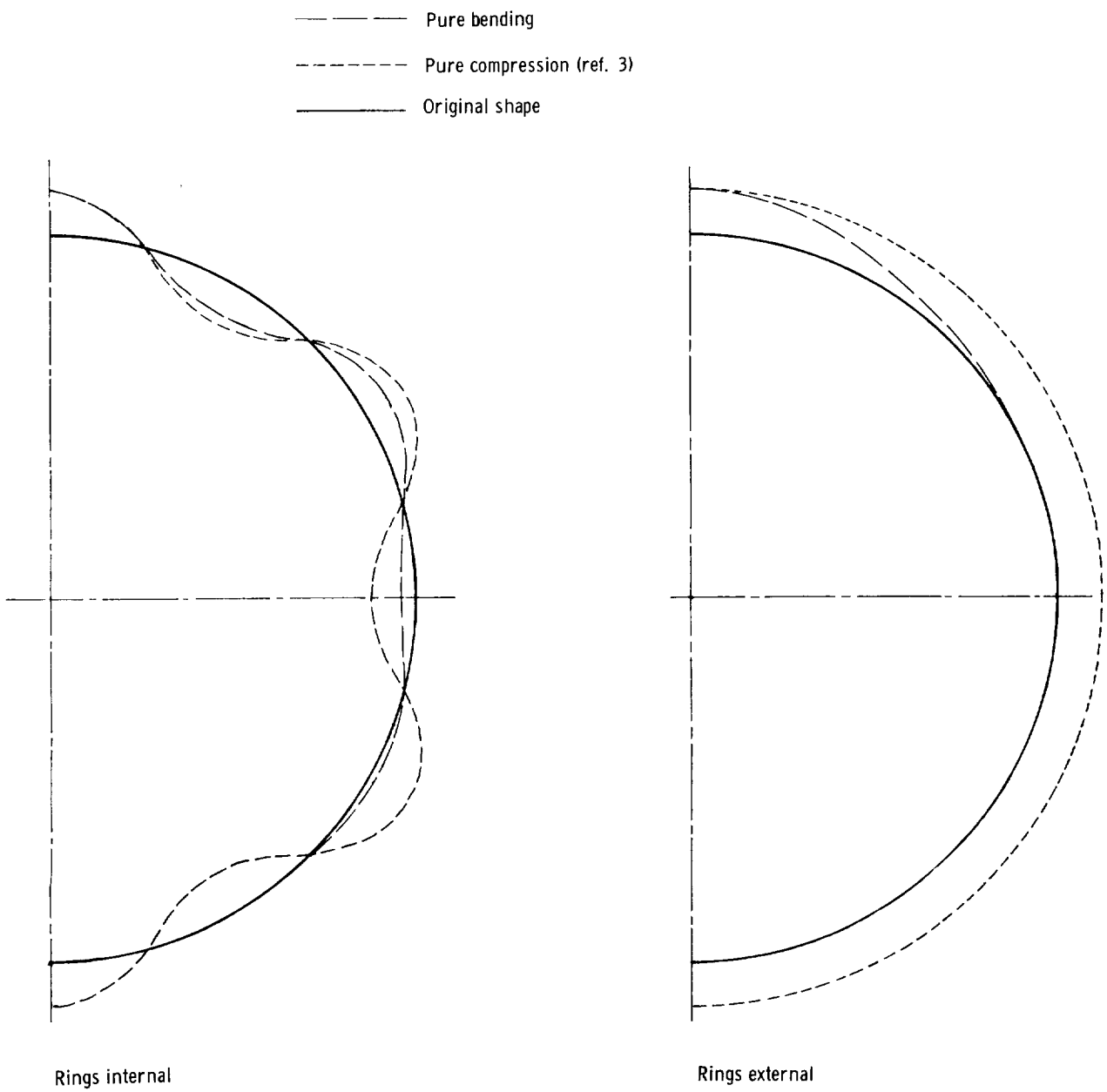

Figure 8.- Predicted mode shapes for ring-stiffened corrugated cylinder with $\ell/R = 0.2$.

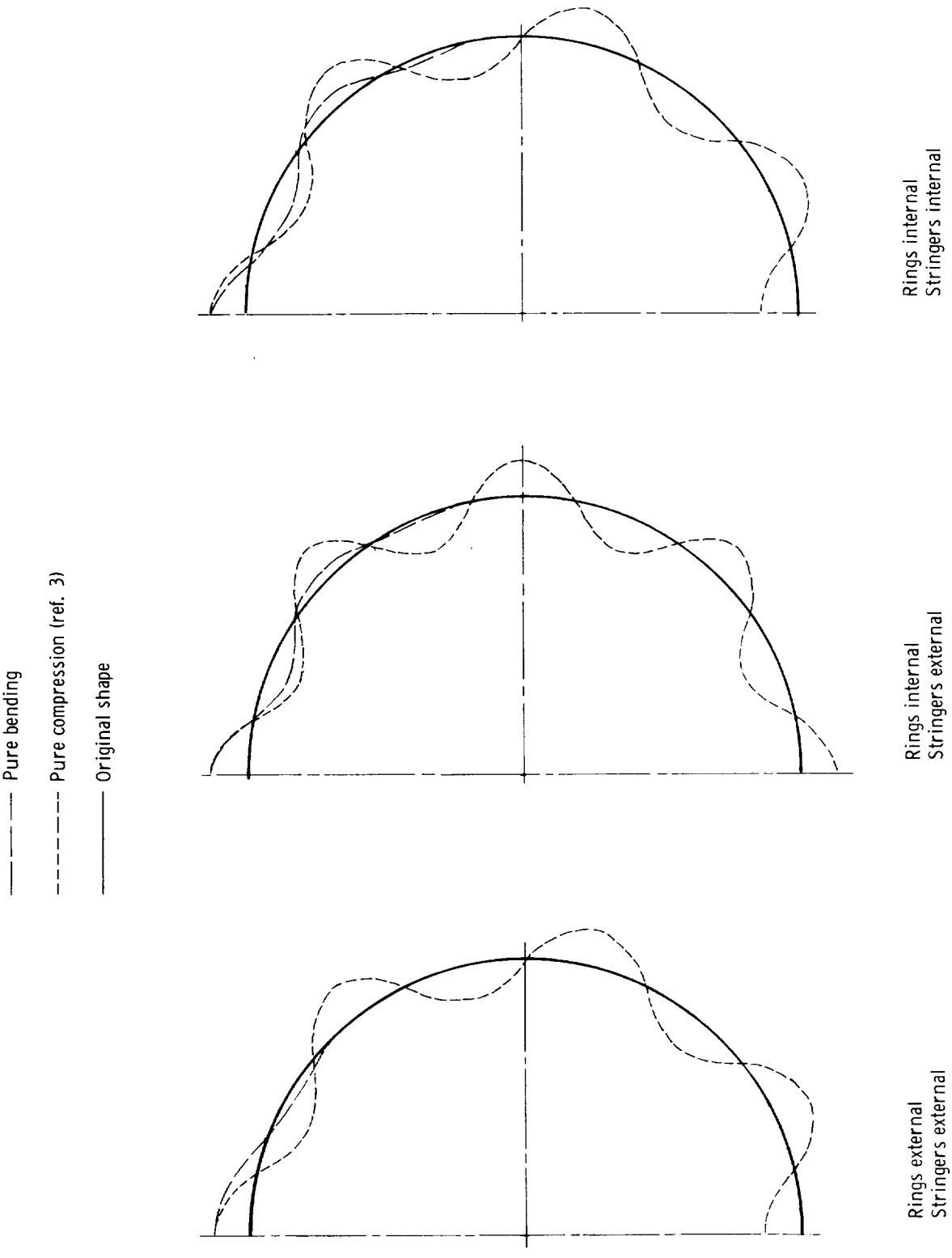

Figure 9.- Predicted mode shapes for ring- and stringer-stiffened cylinder with $l/R = 0.15$.